SUPPLEMENTARY INFORMATION

A dinuclear biomimetic Cu complex derived from L-histidine: Synthesis and stereoselective oxidations

Maria L. Perrone,[a] Elena Salvadeo,[a] Eliana Lo Presti,[a] Luca Pasotti,[a,b] Enrico Monzani,[a] Laura Santagostini,[c] Luigi Casella*[a]

[a]Dipartimento di Chimica, Università di Pavia, Via Taramelli 12, 27100 Pavia, Italy
[b]Noxamet Srl, Dipartimento di Chimica, Università di Pavia, 27100 Pavia, Italy
[c]Dipartimento di Chimica, Università di Milano, 20133 Milano, Italy

Derivation of the kinetic equation for a catalytic reaction requiring the binding of two substrate molecules.

The catalytic oxidations of norepinephrine enantiomers by $[Cu_2(EHI)]^{4+}$ show a substrate sigmoidal dependence suggesting the binding of two substrate molecules to the catalyst in order to observe catalysis. The reaction scheme describing the catalytic behavior is as follow:

$$C + 2S \overset{\beta_2}{\rightleftharpoons} CS_2 \xrightarrow{k_{cat}} \rightarrow\rightarrow C + S + P$$

where C is the catalyst, S is norepinephrine, CS_2 is the catalyst bound to two substrate molecules and P is the product of the reaction.

Assuming that:

a) The binding step I fast with respect to the turnover cycle rate (as shown by the fast binding observed in the binding studies with $[Cu_2(EHI)]^{4+}$ and considering the slow reaction rates, i.e. moderate k_{cat} values)

b) The binding of two substrate molecules is needed to perform the reaction (i.e., the CS species is catalytically not efficient)

c) Only a minor fraction of the complex with bound only one substrate molecule accumulates during turnover (i.e., [CS]<<[C]+[CS_2])

According to point a, the binding of the two substrate molecules occurs as a pre-equilibrium, allowing the use of the binding constant β_2 (equation 1), together with the mass balance on the catalyst (equation 2), to obtain the species concentration during turnover

$$C + 2S \overset{\beta_2}{\rightleftharpoons} CS_2 \qquad \beta_2 = \frac{[CS_2]}{[C]\cdot[S]^2} \tag{1}$$

$$[C]_0 = [C] + [CS_2] \tag{2}$$

where $[C]_0$ is the total (free plus substrate bound) concentrations of the catalyst

$[CS_2]$ can be obtained from equation 1, $[CS_2] = \beta_2 \cdot [C]\cdot[S]^2$

The substitution of $[CS_2]$ in equation 2 gives the free (not bound) catalyst concentration:

$$[C] = \frac{[C_0]}{1 + \beta_2 \cdot [S]^2} \tag{3}$$

And then that of the CS_2 species:

$$[CS_2] = \frac{[C_0]\cdot \beta_2 \cdot [S]^2}{1 + \beta_2 \cdot [S]^2} \tag{4}$$

The reaction rate depends on $[CS_2]$ through equation 5:

$$r = k_{cat} \cdot [CS_2] \tag{5}$$

The rate equation is obtained by combining equations 4 and 5:

$$r = \frac{k_{cat} \cdot [C_0]\cdot \beta_2 \cdot [S]^2}{1 + \beta_2 \cdot [S]^2} \tag{6}$$

and

$$\frac{r}{[C_0]} = \frac{k_{cat} \cdot \beta_2 \cdot [S]^2}{1 + \beta_2 \cdot [S]^2} = \frac{k_{cat} \cdot [S]^2}{1/\beta_2 + [S]^2} = \frac{k_{cat} \cdot [S]^2}{K' + [S]^2} \tag{7}$$

where $K' = 1/\beta_2$

Derivation of the kinetic equation to interpret the monomeric-dimeric equilibrium of $[Cu_2(EHI)]^{4+}$.

In order to model this peculiar behavior, the kinetic equations were appropriately derived with the assumption that, in substrate-saturating conditions, the oxidation rate depends only on complex concentration. We also assume that the complex exists in two forms in dynamic equilibrium, a monomeric and a dimeric species:

$2C \rightleftharpoons C_2$ ruled by $K_b = [C_2]/[C]^2$

Oxidation rate depends from both [C] and $[C_2]$

$r = k_1[C] + k_2[C_2]$

Considering the mass equation:

$[C_0] = [C] + 2K_b[C]^2$

appropriate substitution leads to the final equation, used for the interpolation:

$$r = k_1\left(\frac{-1+\sqrt{1+8\,x\,K_b\,x\,[C_0]}}{4K_b}\right) + k_2K_b\left(\frac{-1+\sqrt{1+8\,x\,K_b\,x\,[C_0]}}{4K_b}\right)^2$$

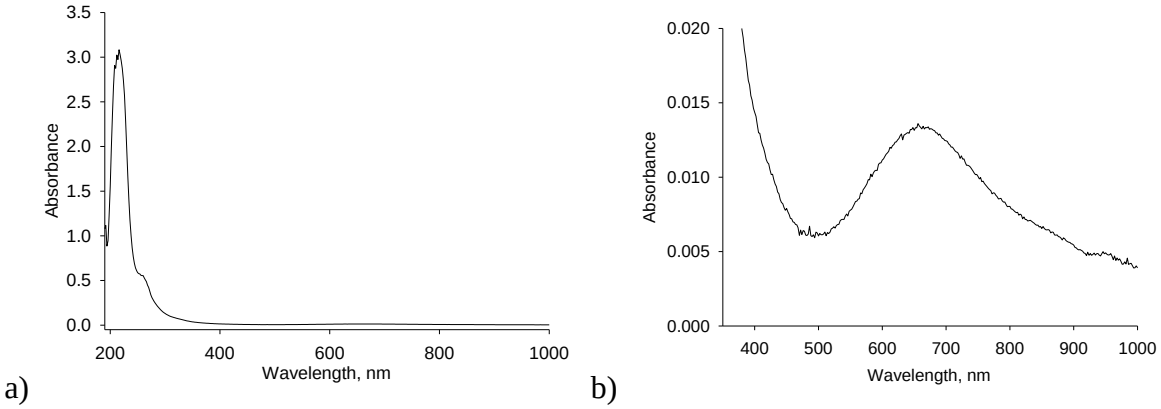

a) b)

Figure 1S. (a) UV-Vis spectra of $[Cu_2(EHI)]^{4+}$ in methanol, 0.1 mM. (b) Magnification of the low energy region.

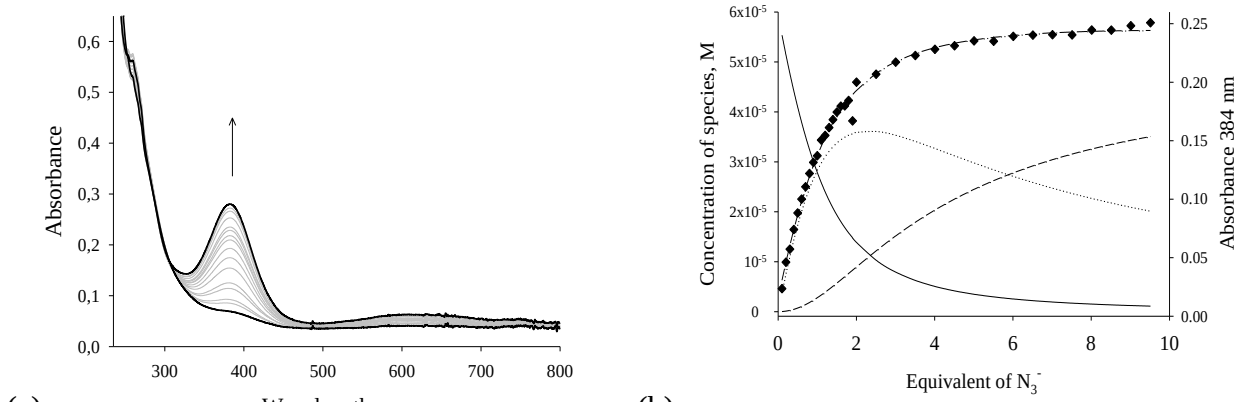

(a) (b)

Figure 2S. (a) Family of UV-Vis spectra taken upon addition of a concentrated solution of NaN_3 to $[Cu_2EHI]^{4+}$ in 9:1 methanol/acetonitrile (v/v) solution. Solid black lines: initial and final spectra of the titration, corresponding to $[Cu_2EHI]^{4+}$ and the mixture of $[Cu_2EHI(N_3)]^{3+}$ and $[Cu_2EHI(N_3)_2]^{2+}$ species, respectively. (b) Distribution diagram (concentration *vs.* equiv. of added NaN_3) of the species, calculated for log K_{b1} = 4.61, and log K_{b2} = 3.59, according to reactions (1) and (2), respectively.

$$[Cu_2EHI]^{4+} + N_3^- \rightleftharpoons [Cu_2EHI(N_3)]^{3+} \quad (1)$$

$$[Cu_2EHI(N_3)]^{3+} + N_3^- \rightleftharpoons [Cu_2EHI(N_3)_2]^{2+} \quad (2)$$

Solid and dotted black lines: free $[Cu_2EHI]^{4+}$ and $[Cu_2EHI(N_3)]^{3+}$, respectively; dashed black line: $[Cu_2EHI(N_3)_2]^{2+}$. The graph shows the experimental profile of absorbance *vs.* equiv. NaN_3 at 385 nm (diamonds) and the fitted curve (dashed line).

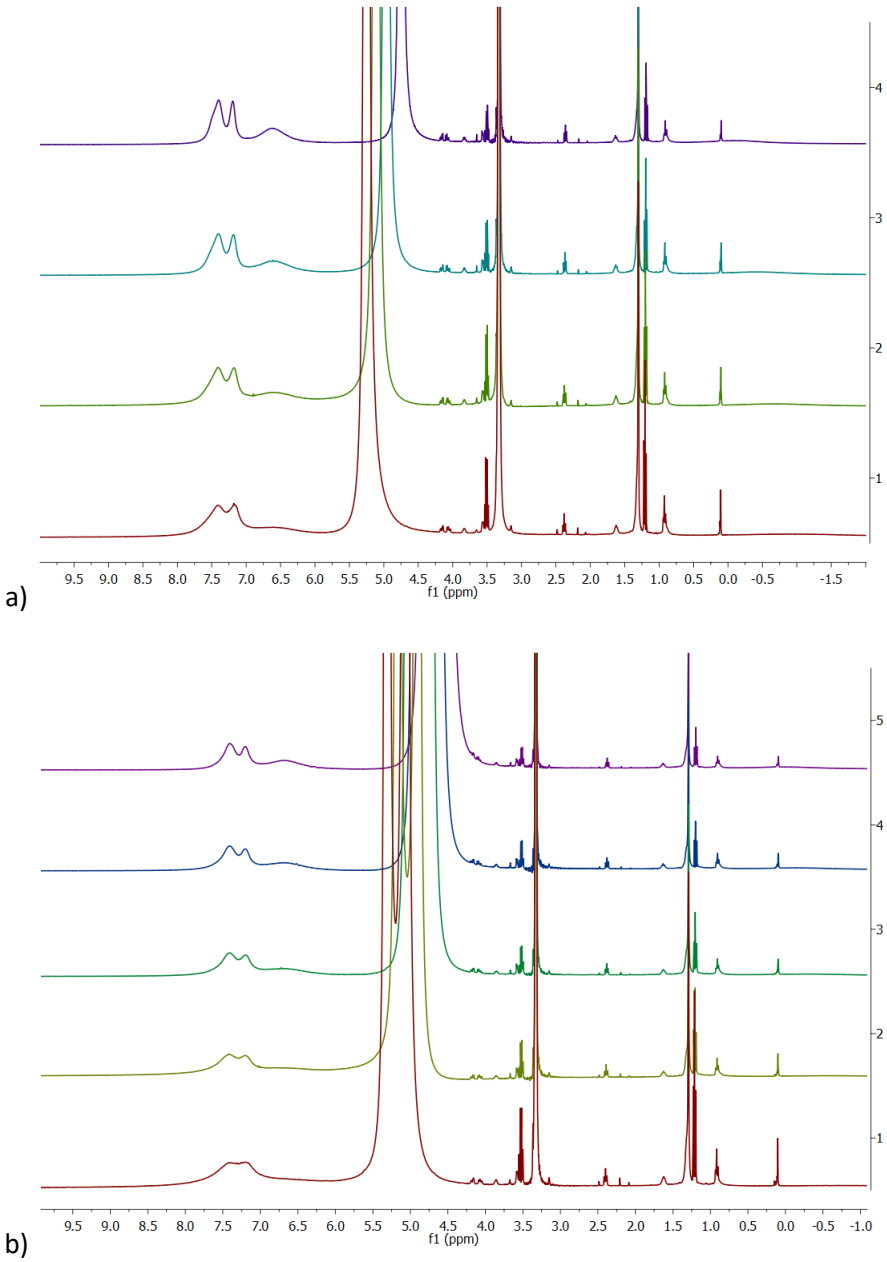

Figure 3S. (a) ^{1}H-NMR spectral variation of a solution of $[Cu_2(EHI)](ClO_4)_4$ (2.2 mM) in deuterated methanol (MeOD) upon increasing the temperature (trace 1: -15 °C; 2: 0 °C; 3: 15 °C; 4: 35 °C); (b) ^{1}H-NMR spectral variation of a solution of $[Cu_2(EHI)](ClO_4)_4$ (1.98 mM) in MeOD/deuterated acetate buffer (50 mM, pH 5.1) 10:1 (v/v) upon increasing the temperature (trace 1: -15 °C; 2: 0 °C; 3: 15 °C; 4: 25 °C; 5: 35 °C).

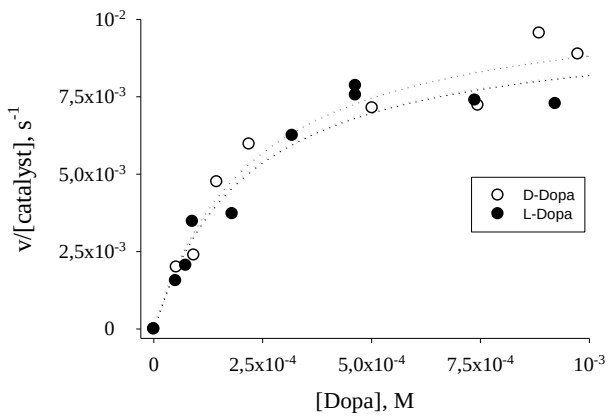

(a)

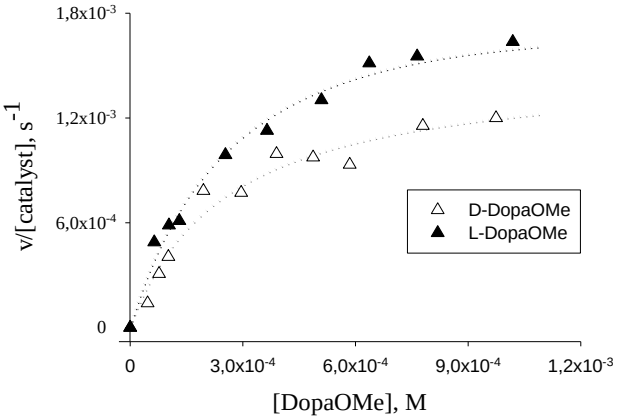

(b)

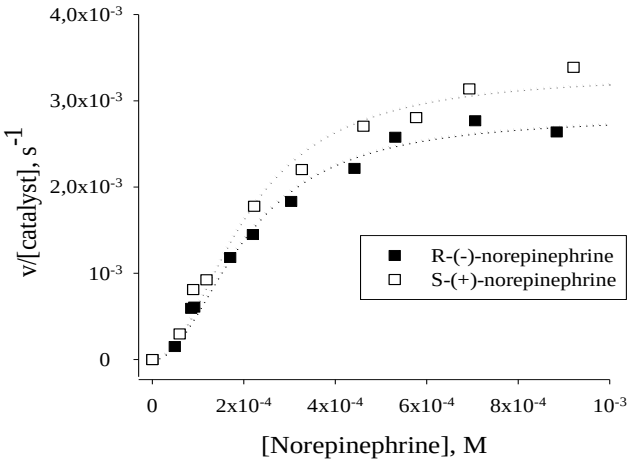

(c)

Figure 4S. Effect of substrate concentration on the initial rate of oxidation of L-/D-Dopa (a), L-/D-DopaOMe (b), and R-/S-norepinephrine (c) by $[Cu_2EHI](ClO_4)_4$ (1 μM) in a 10:1 (v/v) mixture of methanol/aqueous acetate buffer (50 mM) at pH=5.1.

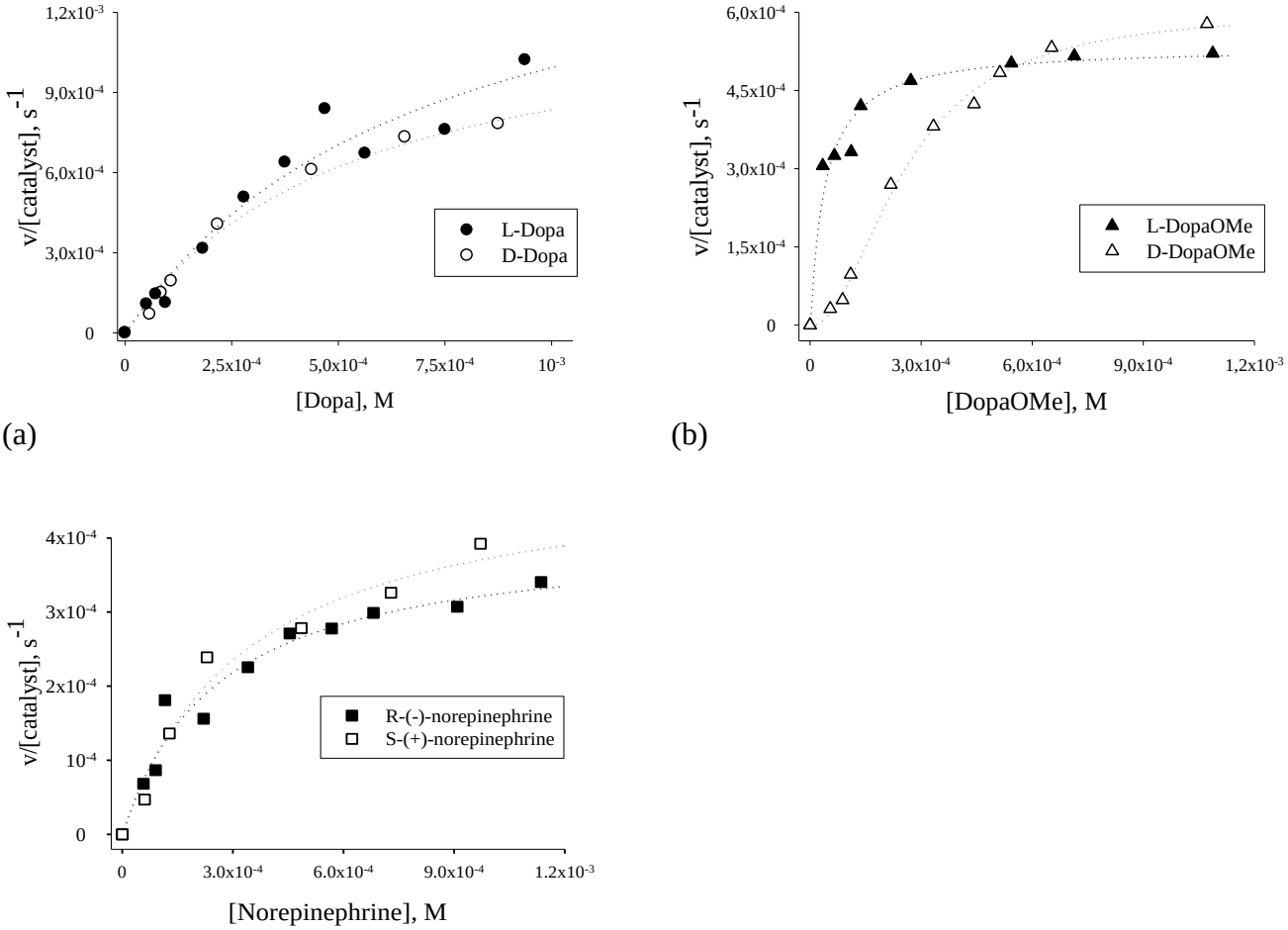

Figure 5S. Effect of substrate concentration on the initial rate of oxidation of L-/D-Dopa (a), L-/D-DopaOMe (b), and R-/S-norepinephrine (c) by $[Cu_2EHI](ClO_4)_4$ (5 μM) in a 10:1 (v/v) mixture of methanol/aqueous acetate buffer (50 mM) at pH=5.1.

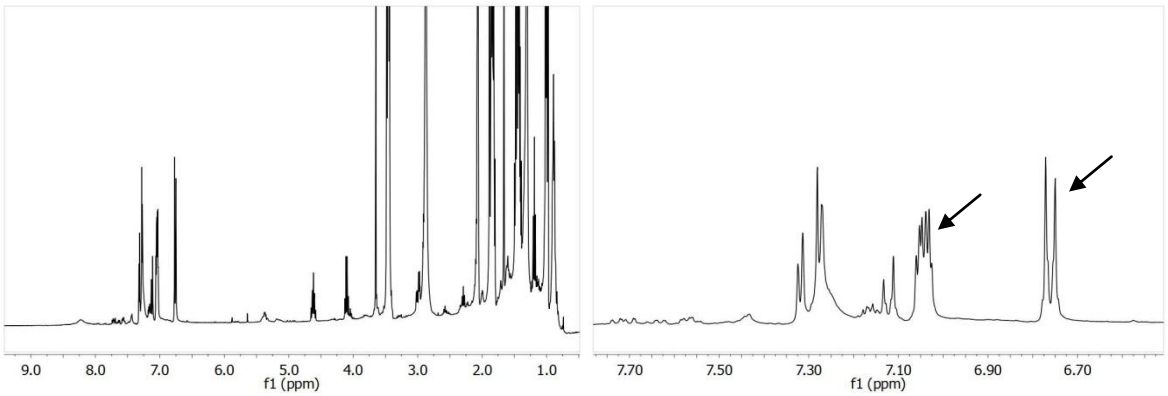

Figure 6S. (Left) ^{1}H NMR spectrum in acetone d-6 (δ values, ppm) of the crude product mixture of hydroxylation reaction of the TBA salt of L-tyrosine. (Right) Expansion of the aromatic region of the spectrum, unreacted phenol signals are indicated with arrows.

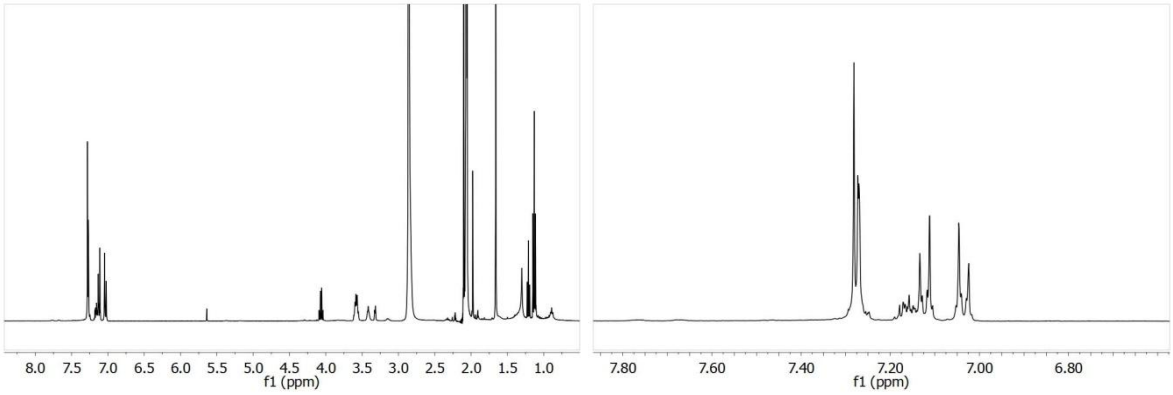

Figure 7S. (Left) ^{1}H NMR spectrum in acetone d-6 (δ values, ppm) of the main product from the hydroxylation reaction of the TBA salt of L-tyrosine. (Right) Expansion of the aromatic region of the spectrum.

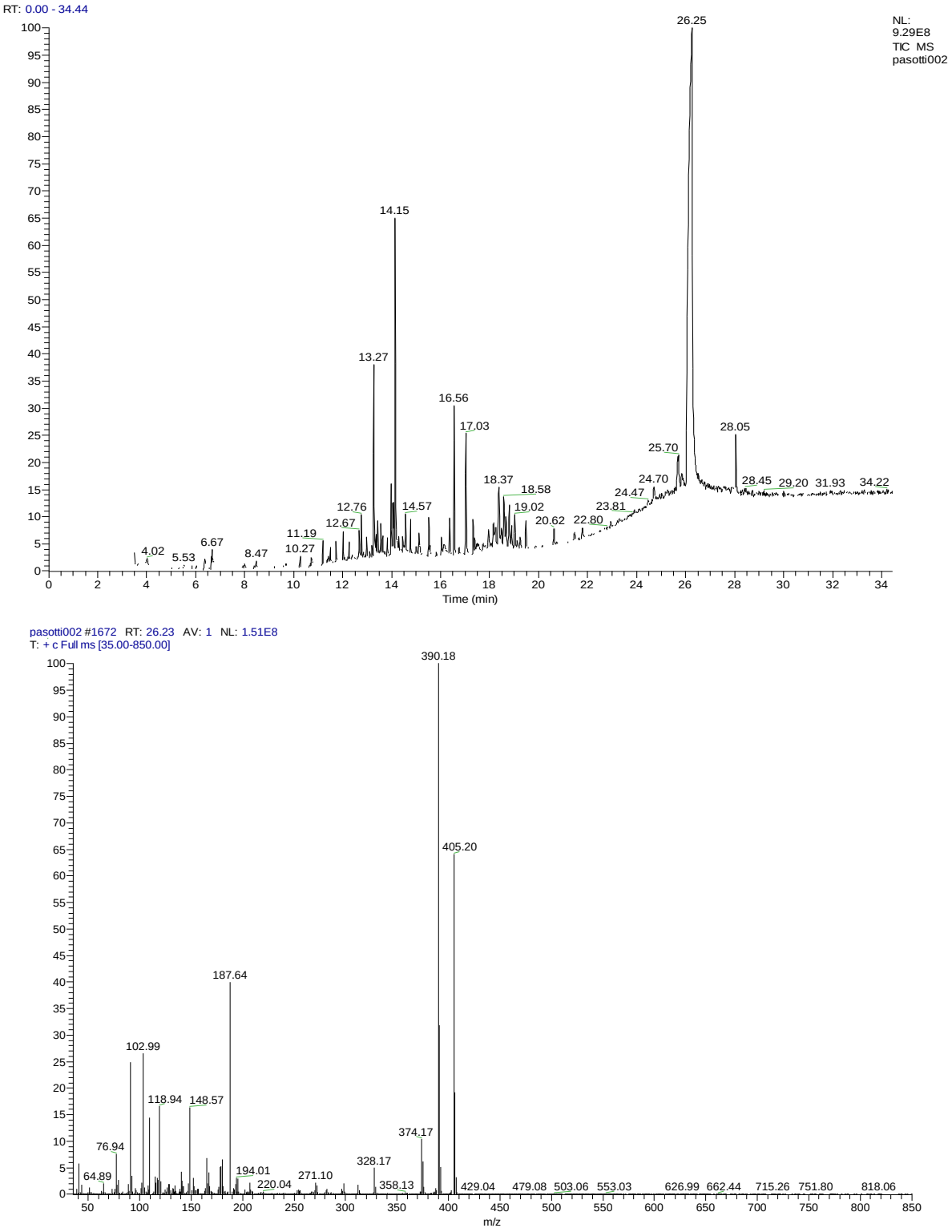

Figure 8S. GC-MS chromatogram of product mixture of the hydroxylation reaction of the TBA salt of L-tyrosine (upper trace) and fragmentation pattern of the main product (bottom trace), with retention time of 26.25 min.

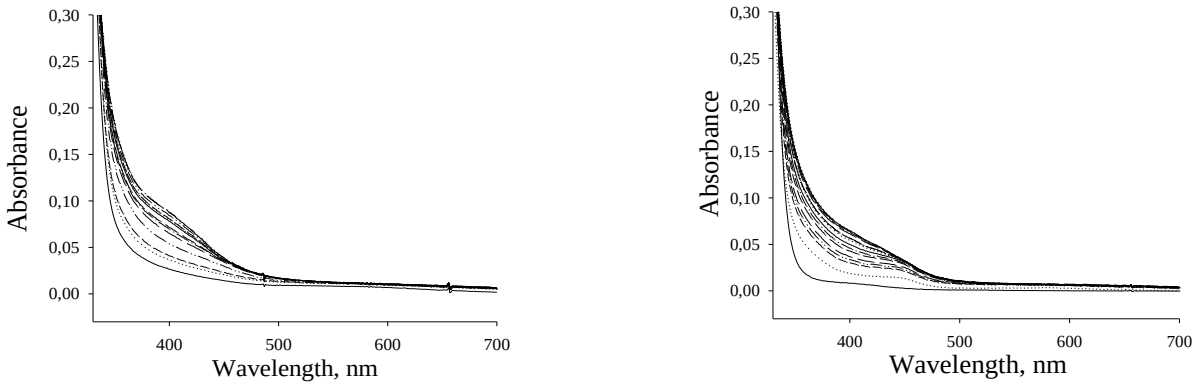

Figure 9S. UV-Vis spectral changes observed during the oxidation of tetrabutylammonium salts of *N*-acetyl-L-tyrosine ethyl ester (left), and *N*-acetyl-D-tyrosine ethyl ester (right) by $[Cu_2(EHI)]^{2+}/O_2$.